

ULTIMATE BEARING CAPACITY OF FOOTING ON SANDY SOIL AGAINST COMBINED LOAD OF VERTICAL, HORIZONTAL AND MOMENT LOADS

Du L. Nguyen¹, S. Ohtsuka², and K. Kaneda³

¹Department of Energy and Environment Engineering, Nagaoka University of Technology, Japan

²Department of Civil and Environmental Engineering, Nagaoka University of Technology, Japan

³Takenaka corporation, Japan

ABSTRACT: Rigid plastic finite element method employing the rigid plastic constitutive equation, which considers non-linear shear strength properties against confining pressure, is used for the assessment of ultimate bearing capacity of footing on sandy soils against the combined load of vertical, horizontal and moment loads. The numerical results were compared with the results predicted by semi-empirical bearing capacity formulae of Architectural Institute of Japan and others. The comparison is conducted in terms of vertical and horizontal loads plane and vertical and moment loads plane. The limit load is expressed in normalization form by the limit vertical load, V_o . Results show that the normalized vertical load decreases with the increase in the normalized horizontal load and/or moment load. Effect of non-linear shear strength on the normalized limit load space in vertical, horizontal and moment loads is clearly indicated. The normalized horizontal load is obtained greater than that of linear shear strength property.

Keywords: Ultimate Bearing capacity, Size effect, Finite element method, Inclined load

1. INTRODUCTION

The ultimate bearing capacity of footing related to inclined loads is an important aspect in geotechnical engineering. Because the number of superstructure buildings has increased and great earthquakes occur regularly, estimating the ultimate bearing capacity of footing with considering the effect of footing width is necessary. The strip footings are often subjected to the inclined loads and the combined loads. The ultimate bearing capacity for combined vertical and horizontal loads (with no moments) is resolved by Green (1954). The general case of vertical, horizontal and moment loads has received less attention. Several authors (notably Meyerhof (1953), Hansen (1970) and Vesic (1975)) provide procedures for a general case; however they only conduct empirical generalizations of the simpler cases without examining in detail. In previous geotechnical research, the combined vertical and horizontal load is referred as the inclined loads. Their results showed that the vertical bearing capacity significantly decreased when the inclined angle $\theta = \tan(H/V)$ increased. By using the ultimate bearing capacity factors N_c , N_q (Prandtl), and N_γ (Meyerhof), the Architectural

Institute of Japan (AIJ, 1988, 2001) developed an ultimate bearing capacity formula which considers the size effect factor and now is widely used in Japan. It was developed by semi-experiments. The ultimate bearing capacity formula is expressed as follows:

$$q_u = i_c \alpha c N_c + i_\gamma \gamma B^\beta N_\gamma + i_q D_f N_q \quad (1)$$

where c : cohesion, γ : unit weight of soil, D_f : depth of embedment, B : footing width; N_c , N_q , N_γ : bearing capacity factors; i_c , i_q , i_γ : inclination factors, α and β express the shape coefficient and $\alpha = 1$ and $\beta = 0.5$ are recommended by De Beer (1970), respectively; q_u is ultimate vertical bearing capacity per unit area of footing (kN/m^2). η : the size effect factor is defined as:

$$\eta = \left(\frac{B}{B_o} \right)^m \quad (2)$$

where, B_o : reference value in footing width
 m : coefficient determined from the experiment ($m = -1/3$ is recommended in practice).

Meyerhof (1956) introduced 'inclination factor i_γ ' that is defined as follows:

$$i_\gamma = \frac{V}{V_o} = \left(1 - \frac{\tan(H/V)}{\phi} \right)^2 \quad (3)$$

where ϕ : internal friction angle, H and V : horizontal and vertical of the load applied on the footing, V_o : vertical ultimate load.

Inclination factor has been estimated by FE analysis. But, there are few analyses for sandy soils except Loukidis et al. (2008). However, the effect of footing width on ultimate bearing capacity is not considered directly. As shown in Eqs. (1) and (2), the size effect of footing is large in case of sandy soil. It can be seen in the combined load space of vertical, horizontal and moment loads. This is a major topic of this study. Recently, the numerical methods are efficient techniques for solving problems related to geotechnical engineering. The rigid-plastic finite element method (RPFEM) was applied in geotechnical engineering by Tamura (1991). In this process, the limit load is calculated without the assumption about the potential failure mode. The method is effective in calculating the ultimate bearing capacity of footing against the three-dimensional boundary value problems. Although RPFEM was originally developed based on the upper bound theorem in plasticity, Tamura proved that it could be derived directly by using the rigid plastic constitutive equation.

This paper investigated the ultimate bearing capacity of footing on sandy soils against the combined load of vertical, horizontal and moment loads. This research applied rigid plastic finite element method which employs the rigid plastic constitutive equation in which non-linear shear strength properties against confining pressure is included. The vertical load V , horizontal load H and moment M , which were applied at the center of the footing, were subjects in this study. The analytical method provides the reliable computational results. The relation in normalization form of H/V_o vs V/V_o and V/V_o vs M/BV_o were acquired and then were compared with the relationship by Meyerhof (1956), Architectural Institute of Japan (1988, 2001) and Loukidis et al. (2008).

2. RIGID PLASTIC FINITE ELEMENT METHOD

2.1 Stress – Strain rate relationship

Tamura (1987, 1991) developed the rigid plastic constitutive equation for the frictional material whose strength satisfies the Drucker-Prager yield criterion:

$$f(\sigma) = aI_1 + \sqrt{J_2} - b = 0 \quad (4)$$

where I_1 : first stress invariant

J_2 : second invariant of deviator stress S_{ij}

The coefficients a and b express the soil constants corresponding to the internal friction angle and cohesion, respectively.

The volumetric strain rate is expressed as follows:

$$\begin{aligned} \dot{\epsilon}_v &= \text{tr}(\dot{\epsilon}) = \text{tr}\left(\lambda \frac{\partial f(\sigma)}{\partial \sigma}\right) \\ &= \text{tr}\left(\lambda \left(\alpha \mathbf{I} + \frac{\mathbf{s}}{2\sqrt{J_2}}\right)\right) = \frac{3a}{\sqrt{3a^2 + 1/2}} \dot{\epsilon} \end{aligned} \quad (5)$$

where λ : the plastic multiplier, and $\dot{\epsilon}$: the norm of strain rate. \mathbf{I} and \mathbf{s} express the unit and the deviatoric stress tensors. The strain rate $\dot{\epsilon}$, which is purely plastic component, should satisfy the volumetric constraint condition which is derived by Eq. (5) as follows:

$$h(\dot{\epsilon}) = \dot{\epsilon}_v - \frac{3a}{\sqrt{3a^2 + 1/2}} \dot{\epsilon} = \dot{\epsilon}_v - \hat{\eta} \dot{\epsilon} = 0 \quad (6)$$

Each strain rate, which is compatible with Drucker-Prager's yield criterion, must satisfy the kinematical constraint conditions of Eq. (6). $\hat{\eta}$ is a coefficient determined by Eq. (6) which is on the dilation characteristics. The rigid plastic constitutive equation is expressed by Lagrangian method after Tamura (1991) as follows:

$$\sigma = \frac{b}{\sqrt{3a^2 + \frac{1}{2}}} \frac{\dot{\epsilon}}{\dot{\epsilon}} + \hat{\beta} \left(\mathbf{I} - \frac{3a}{\sqrt{3a^2 + \frac{1}{2}}} \frac{\dot{\epsilon}}{\dot{\epsilon}} \right) \quad (7)$$

The first term expresses the stress component uniquely determined for the yield function, and the second term expresses the indeterminate stress component, defined to be parallel to one of the generators of the cylindrical cone of the yield surface. The indeterminate stress parameter $\hat{\beta}$ still remains unknown until the boundary value problem with Eq. (6) is solved.

In this study, the constrain condition on strain rate is introduced into the constitutive equation directly with the use of penalty method:

$$\sigma = \frac{b}{\sqrt{3a^2 + \frac{1}{2}}} \frac{\dot{\epsilon}}{\dot{\epsilon}} + \kappa(\dot{\epsilon}_v - \hat{\eta} \dot{\epsilon}) \left(\mathbf{I} - \frac{3a}{\sqrt{3a^2 + \frac{1}{2}}} \frac{\dot{\epsilon}}{\dot{\epsilon}} \right) \quad (8)$$

where, κ is a penalty constant. This technique makes the computation more stable and faster. In rigid plastic finite element method (RPFEM), the occurrence of zero energy modes has been pointed out and some numerical techniques to avoid it have been introduced into FEM. However, zero energy modes have not been observed in computation with the rigid plastic constitutive equation using the Penalty method.

2.2 Rigid plastic constitutive equation for non-linear shear strength property

Tatsuoka (1986), and other researchers (Hettler, A. and Gudehus, G. (1988)) reported the effects of confining pressure on the internal friction angle for sandy soils by experiments. The property of the normalization between internal friction angle and first stress invariant always holds irrespective of the reference value of the confining pressure in the standardization of internal friction angle (Du N. L. et al. (2013)). From Fig. 1, the obtained results from experiment on Toyoura sand, Degebo sand, Eastern Scheldt sand, and Darmstadt sand indicated that although internal friction angles are different between soils, the normalized internal friction angle shows the same trend for all case studies although any reference values of ϕ_0 and I_1 are employed in normalization form. Thus, non-linear shear strength property against confining pressure is included in RPFEM in order to assess the ultimate bearing capacity of footing on sandy soils by taking account of the size effect of footing. The internal friction angle $\phi = 30^\circ$ at I_1 as 150 kPa is employed as references through the following case studies.

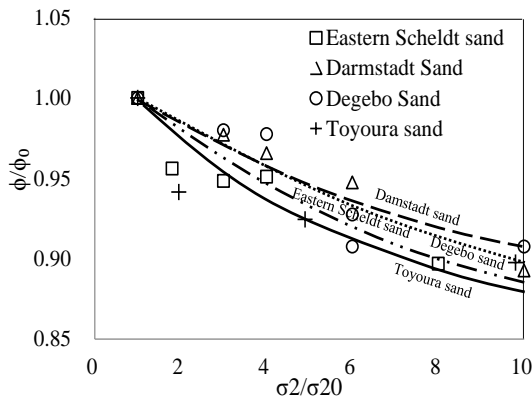


Fig. 1 Relationship between internal friction angle and first stress invariant for various kinds of sands

The high order hyperbolic function is introduced to the yield function of sandy soils as follows:

$$f(\sigma) = aI_1 + (J_2)^n - b = 0 \quad (9)$$

where a and b are the soil constants. The index n expresses the degree in non-linearity in shear strength against the first stress invariant. Eq. (9) is identical with Drucker-Prager yield function in case of $n=1/2$. The non-linear parameters a , b and n are identified by the testing data. In this case studies, $a = 0.24$, $b = 2.4$ kPa and $n = 0.56$ was set based on the experiment data from Fig. 1.

The non-linear rigid plastic constitutive equation for confining pressure is obtained as follows:

$$\sigma = \frac{3a}{n} \left\{ \frac{I}{2n^2} \left[\left(3a \frac{\dot{\epsilon}}{\dot{\epsilon}_v} \right)^2 - 3a^2 \right] \right\}^{\frac{1-n}{2n-1}} \frac{\dot{\epsilon}}{\dot{\epsilon}_v} + \left[\frac{b}{3a} - \frac{I}{3a} \left[\frac{I}{2n^2} \left(3a \frac{\dot{\epsilon}}{\dot{\epsilon}_v} \right)^2 - 3a^2 \right]^{\frac{n}{2n-1}} \right] \left[-\frac{a}{n} \left[\frac{I}{2n^2} \left(3a \frac{\dot{\epsilon}}{\dot{\epsilon}_v} \right)^2 - 3a^2 \right]^{\frac{1-n}{2n-1}} \right] \mathbf{I} \quad (10)$$

Stress is uniquely determined for plastic strain rate and it is different from Eq. (8) for Drucker-Prager yield function in this equation.

The authors successfully proposed a rigid plastic equation using non-linear shear strength property against confining stress to RPFEM to assess the ultimate bearing capacity for the vertical load cases of rigid flat footing (Du N. L. et al. (2013)). The results of RPFEM were obtained similarly to the ultimate bearing capacity formula by Architectural Institute of Japan (AIJ, 1988, 2001), which take into account the size effect of footing.

3. ULTIMATE BEARING CAPACITY OF FOOTING UNDER COMBINED LOADS

3.1 Ultimate bearing capacity for combined vertical and horizontal loads

The rigid plastic finite element method was used to assess the ultimate bearing capacity of strip footings of which the width varied from 1m to 100m, subjected to the inclined load at an inclination angle θ with respect to the vertical. The boundary conditions and typical mesh for analysis are shown in Fig. 2.

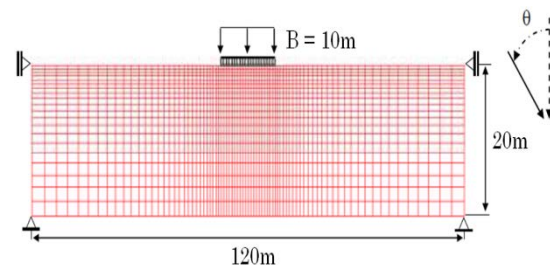


Fig. 2 Typical finite element mesh and boundary conditions

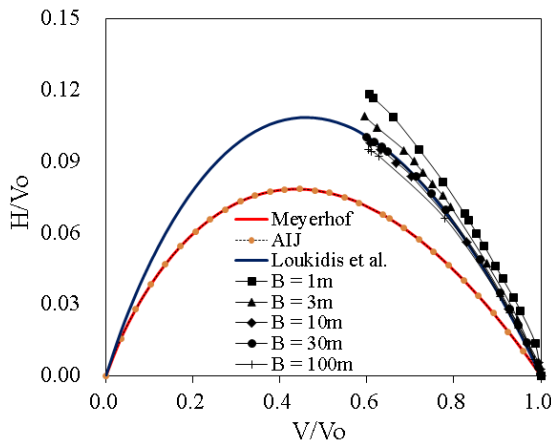
Because of the absence of loads symmetry, the entire soil domain of dimensions will be considered. The numerical simulation procedure was used for the computation of the (H, V) failure envelope (where H and V are the horizontal and vertical ultimate footing loads, respectively).

For inclined load, the application of RPFEM is limited to the case where the contact pressure between footing and ground is positive. In other words, the ratio H/V is set comparatively in small range. Further detailed discussion will not be conducted in this study.

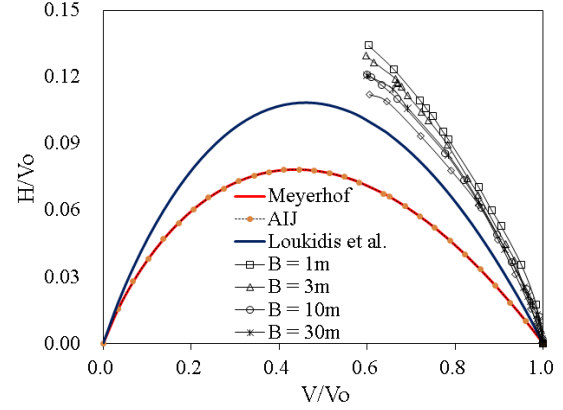
Fig. 3 provides the RPFEM result on the relationship between normalized horizontal and vertical loads on H/V space. Two cases considered include (i) linear shear strength property and (ii) non-linear shear strength property. The results by AIJ and Meyerhof formulae are also shown. Since AIJ formula employs the same coefficient with Meyerhof method, the results in normalization form from AIJ and Meyerhof show unique and coincident line. The inclination coefficient proposed by Loukidis et al. (2008) is also shown in this figure. They proposed the inclination factor i_γ based on the FE analysis for $B=10\text{m}$ as follows:

$$i_\gamma = \frac{V}{V_0} = \left(1 - \frac{(H/V)}{\tan \phi}\right)^{(1.5 \tan \phi + 0.4)^2} \quad (11)$$

This coefficient is developed for linear shear strength, but it differs from the lines of Meyerhof and AIJ as shown in Fig. 3a. In the figure, the normalized horizontal load is indicated greater than those of Meyerhof and AIJ. The obtained results by RPFEM are plotted for various footing widths. It is apparent that the results match with the model of Eq. (11) by Loukidis et al. though they are varied for footing width.



a) RPFEM with linear shear strength property



b) RPFEM with non-linear shear strength property

Fig.3 The relation between normalized horizontal and vertical loads

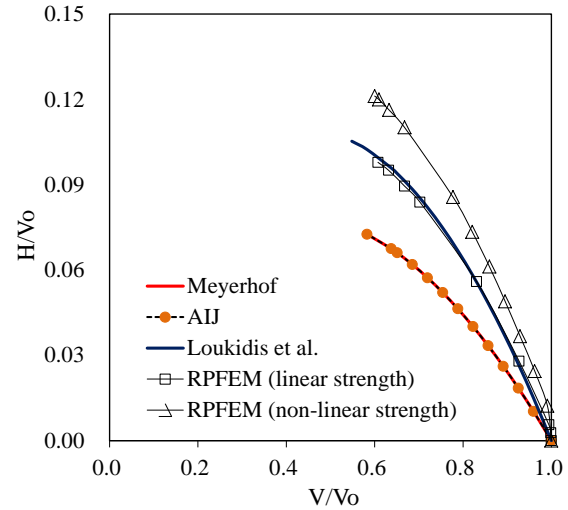
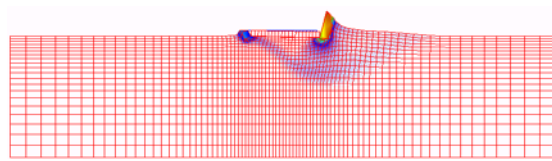


Fig. 4 Comparison inclination coefficients among the various methods at footing width $B = 10\text{m}$

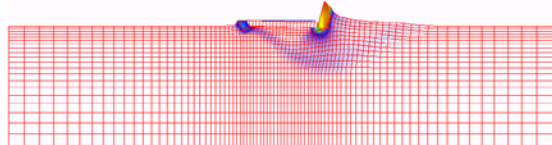
Fig. 3b indicates the inclination coefficient in case of non-linear shear strength. AIJ formula is developed by taking account of the size effect of footing. However, since the inclination coefficient of Meyerhof is introduced into the formula, the applicability of AIJ formula for inclined load has not been examined. The results by RPFEM taking account of non-linear shear strength are plotted in the figure. Fig.4 indicates the ultimate load in H/V_0 and V/V_0 space to compare the inclination coefficient among the various methods at $B=10\text{m}$. It is readily seen that RPFEM affords the identical results by Loukidis et al. in case of linear shear strength, but the greater results than that by Loukidis et al. in case of non-linear shear strength. Although ϕ is constant in case of linear shear strength, ϕ decreases by confining pressure in case of non-linear shear strength. Since the decrease in

ϕ mostly depends on the magnitude of vertical load, the decrease in ultimate bearing capacity is largest for vertical loading. For the inclined load, the decrease in ϕ becomes moderate with the increase in inclination angle of inclined load. It derives the normalized horizontal load in case of non-linear shear strength greater than that of linear shear strength.

Fig. 5 showed the failure modes of ground for non-linear and linear shear strength. They are similar, but the deformation area in the case of linear shear strength is larger than that in case of the non-linear shear strength. The mechanism is found composed of three different zones and similar to the mechanism assumed by Meyerhof and Hansen.



a) RPFEM with linear shear strength property



b) RPFEM with non-linear shear strength property

Fig. 5 Deformation mechanism analysis at footing width $B = 10\text{m}$

3.2 Ultimate bearing capacity for vertical, horizontal and moment loads

The type of loads, which is often known as combined loads, is important to the stability of superstructure where footings are subjected to vertical, horizontal and moment loads combination. Typically, the vertical force is stemmed from the weight (W) of superstructure, while the horizontal load comes from the seismic coefficient H/V , and the overturning moment load is caused by the horizontal load. In case study, vertical loads range from about 150 kN to 300 kN and the overturning moment varies from 200 kN.m to 500 kN.m. A series of finite element analysis were conducted for sandy soil with unit weight $\gamma = 18 \text{ kN/m}^3$, cohesion $c = 5 \text{ kN/m}^2$, internal friction angle $\phi = 30^\circ$, the height of superstructure h (10-20m), and at the footing width $B = 3\text{m}$. The moment load is given to the footing by the external force where the summations in vertical and horizontal loads are zero and the resultant moment at the center of footing is same with the prescribed moment load. The results demonstrated the interaction between

the vertical, horizontal and moment loads. Fig. 6 shows the representative finite element meshes of analysis.

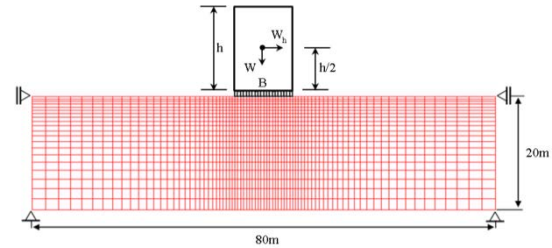
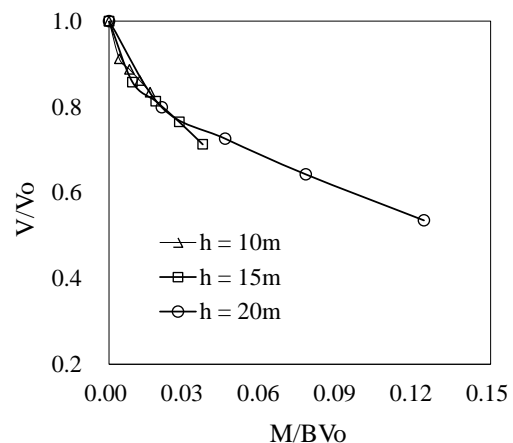
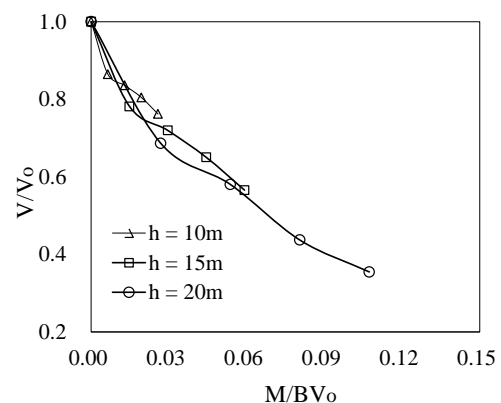


Fig. 6 Representative finite element meshes under superstructure on the strip footings condition at 3m of footing width

At each height of superstructure value, the ultimate bearing capacity of footings subjected to combined loading was computed under the condition of seismic load applied to superstructure. By changing superstructure height and the seismic coefficient H/V , the forces H , and V the moment load was computed.



a) Linear shear strength property

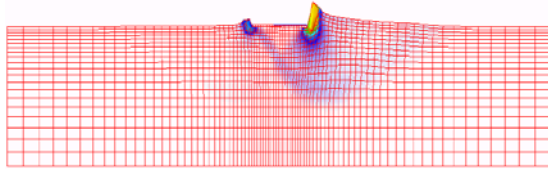


b) Non-linear shear strength property

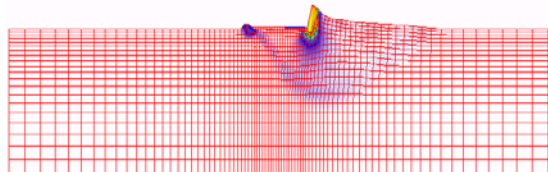
Fig. 7 The relation between normalized vertical and moment loads

Fig. 7 shows ultimate bearing capacity of footing failure in the normalized V-M form by changing superstructure height (10m, 15m and 20m). The results showed that the normalized load V/V_0 decreases with an increase in M/BV_0 . In the case of linear strength, the values that represent the relationship between the normalized V/V_0 and M/BV_0 are similar. It is not affected by height of superstructure; while in case of non-linear strength those values are discrepancy. It is explained that this case influences the internal friction angle responding to the confining stress. It means that the effect of moment load in non-linear case is clearer than that in linear shear strength property. Fig. 8 shows examples of the deformation mechanism from evaluates at the collapse. The larger the combination loads, the smaller the limit load. The results from analysis computation also show that the failure mechanism is asymmetrical and confined to one side of the footing.

$H/V = 0.1$

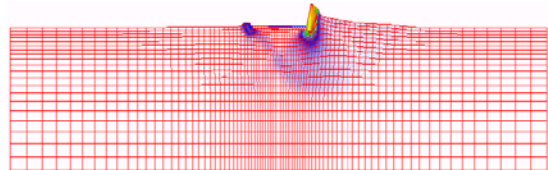


$H/V = 0.4$

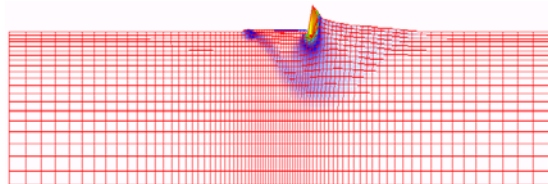


a) Linear shear strength property

$H/V = 0.1$



$H/V = 0.4$



b) Non-linear shear strength property

Fig. 8 Deformation mechanism analysis subjected to combined loads

4. CONCLUSION

In this study, the limit load in ultimate bearing capacity is expressed in normalization form. The ultimate bearing capacity of footing that is subjected to the inclined loads and the combined loads of strip footing has been investigated in this study. The obtained conclusions can be summarized as follows:

(1) The non-linear shear strength model for sandy soil is employed in RPFEM to evaluate the size effect of footing on ultimate bearing capacity. Through the case studies the applicability of the method was clearly exhibited.

(2) Ultimate load space in normalized vertical and horizontal loads was shown to match with that by Loukidis et al. (2008) and be greater than those by Meyerhof (1956) and AIJ (1988, 2001) in case of linear shear strength.

On the contrary, it is obtained greater than that by Loukidis et al. in case of non-linear shear strength. It is understood by the following reasons:

(i) The internal friction angle decreases by confining pressure and the decrease is the most for the case of vertical loading.

(ii) In inclined loading, the decrease in internal friction angle becomes smaller since the ultimate vertical load decreases with the increase in inclination angle. Thus, the computed results can be obtained.

(3) The combination of vertical, horizontal and moment loads is considered to evaluate the stability of buildings during earthquake. The effect of moment load on ultimate bearing capacity is investigated through case studies.

5. REFERENCES

- [1] Architectural Institute of Japan, AIJ (1988, 2001), "Recommendations for design of building foundations", 430p.
- [2] Du, N. L., Ohtsuka, S., Hoshina, T., Isobe, K. and Kaneda, K. (2013) "Ultimate bearing capacity analysis of ground against inclined load by taking account of non-linear properties of shear strength", Int. Journal of GEOMATE, Vol. 5, No. 2, pp. 678–684.
- [3] De Beer, E. E. (1970), "Experimental determination of the shape factors and the ultimate bearing capacity factors of sand", Geotechnique, Vol. 20, No. 4, pp. 387 – 411.
- [4] Hettler, A. and Gudehus, G. (1988), "Influence of the foundation width on the ultimate bearing capacity factor", Soils and Foundations, Vol. 28, No. 4, pp. 81-92.

- [5] Loukidis, D., Chakraborty T., and Salgado R., (2008), "Bearing capacity of strip footings on purely frictional soil under eccentric and inclined loads". *Can. Geotech. J.*, Vol. 45, pp. 768-787.
- [6] Meyerhof, G. G. (1956), "Rupture surfaces in sand under oblique loads (discussion)", *Journal of soil mechanics and foundations division, ASCE*, Vol. 82, No. SM3.
- [7] Tamura, T., Kobayashi, S. and Sumi, T. (1987), "Rigid Plastic finite element method for frictional materials", *Soils and Foundations*, Vol. 27, No. 3, pp. 1-12.
- [8] Tamura, T. (1991), "Rigid plastic finite element method in Geotechnical engineering", *Current Japanese Materials Research*, Vol. 7, Elsevier Applied Science, London, pp. 135-164
- [9] Tatsuoka, F., Sakamoto, M., Kawamura, T. and Fukushima, S. (1986), "Strength and deformation characteristics of sand in plane strain compression at extremely low pressures", *Soils and Foundations*, Vol. 26, No. 1, pp. 65– 84.

Int. J. of GEOMATE, Feb., 2016, Vol. 10, No. 1 (Sl. No. 19), pp. 1649-1655.

MS No. 5218j received on Aug.25, 2015 and reviewed under GEOMATE publication policies. Copyright © 2016, International Journal of GEOMATE. All rights reserved, including the making of copies unless permission is obtained from the copyright proprietors. Pertinent discussion including authors' closure, if any, will be published in Feb. 2017 if the discussion is received by Aug. 2016.

Corresponding Author: **Du L. Nguyen**
